16th World Conference on Earthquake, 16WCEE 2017

Santiago Chile, January 9th to 13th 2017

Paper N° 283

Registration Code: S-G1461918601

EFFECTIVE STRESS SIMULATION OF LIQUEFACTION-INDUCED BUILDING SETTLEMENTS

Y. Hong[(1)], Y. Lu[(2)], R.P. Orense[(3)]

[(1)] *Graduate Student, Department of Civil & Environmental Engineering, University of Auckland, yhon905@aucklanduni.ac.nz*
[(2)] *Graduate Student, School of Engineering and Mathematical Sciences, La Trobe University, 18217027@students.latrobe.edu.au*
[(3)] *Associate Professor, Department of Civil & Environmental Engineering, University of Auckland, r.orense@auckland.ac.nz*

Abstract

Earthquake-induced liquefaction has long been recognized as one of the most serious seismic hazards. Damages to residential houses and commercial buildings have been observed following major earthquakes, such as the 2010-2011 Canterbury Earthquake sequence, as a result of loss in bearing capacity of the foundation ground induced by soil liquefaction. These damages include building settlement and foundation tilt (or differential settlement), which are known to affect the function of these structures.

In this paper, numerical modeling and analyses were performed to examine liquefaction-induced settlement of buildings and to investigate the effects of various parameters in inducing settlements. The finite element effective stress analysis software FLIP, developed in Kyoto University, was used for this purpose. The primary objectives of this paper are: (1) to evaluate the settlement and tilt of buildings due to earthquake-induced liquefaction through numerical simulation; and (2) to quantify the effects of different parameters, such as the aspect ratio, the peak ground acceleration, and the thickness of the liquefiable layer on the magnitude of settlement.

Firstly, the models adopted were validated through the results of centrifuge tests available in the literature. Next, various parameters which were deemed to contribute to the magnitude of total and differential settlements were analysed for a specified earthquake motion, with emphasis on the mechanism which induced the damage. These include building height, footing width, peak base acceleration and thickness of liquefiable layers. From the results, clear variation trends of building settlements and foundation rotation/tilt were observed as functions of the above parameters. The trends were expressed in terms of empirical formulas to describe the relationships of the most significant parameters and the resulting building movements.

The results of the parametric study illustrated that taller buildings undergo stronger rocking and generate larger vertical deviatoric stress than shorter buildings and, with the increase in building height, liquefaction-induced building settlement and foundation rotation are exacerbated. Both vertical settlement and foundation rotation decrease with the increase in building width. In addition, while the normalised settlement increases linearly with the peak base acceleration, both the maximum and residual foundation rotations appear to increase dramatically with the peak base acceleration. Finally, using the results obtained, the earlier results available in the literature showing the relation between normalised building settlement and normalised foundation width were re-assessed and new chart was proposed.

Keywords: earthquake; liquefaction; building settlement; foundation rotation; numerical simulation

1. Introduction

The phenomenon of soil liquefaction following major earthquakes has been studied by many researchers for years [1, 2]. Liquefaction has been commonly defined as one involving saturated loose cohesionless material losing much of its strength when subjected to rapid undrained cyclic loading. The catastrophic consequences caused by liquefaction have occurred following many major earthquakes [3] and these include significant settlement, lateral spreading, and foundation failure. Among these effects, settlement of foundation ground and the structure constructed on top of it is perhaps one of the most serious ones that engineers should consider. However, due to the constraints and limitations of laboratory-based experiments, most estimations of building settlements induced by soil liquefaction are based on empirical equations or rules-of-thumb that were developed to estimate post-liquefaction consolidation settlement for the free-field conditions, and such free-field condition is surely different from the ones underneath buildings which are barely investigated in the literature. Moreover, the geometric/structural properties of the building have influence on the resulting settlements, but the extent of such effects has not yet been well-explained [4, 5, 6]. Additionally, other input parameters such as deviatoric strains resulting from soil-structure interaction (SSI)-induced building ratcheting, input ground motion intensity and building geometry are not taken into account when analysing free-field condition. The development of excess pore water pressure which could induce changes in the ground motion has not been considered directly in the current procedures [7, 8].

Furthermore, laboratory physical model experiments, such centrifuge tests, have been widely adopted to identify the effects of critical parameters, including the inertia forces on the structures and drainage speed [9, 10]. Numerical simulations have also been used to evaluate the basic relationships between the magnitude of building settlement and various factors, such as footing width and thickness of the liquefiable layer [11, 12, 13, 14]. However, very limited information about the fundamental mechanism of liquefaction-induced building movements has been provided and none of them considered the foundation rotation effect, which is obviously an important factor. It has been well-accepted that it is the differential (non-uniform) settlement, and not the total settlement, which may actually determine whether the damage to a building is acceptable or not.

The main objectives of this paper are: (1) to evaluate the settlement and tilt of buildings that suffer from earthquake-induced liquefaction through numerical simulation; and (2) to quantify the effects of different parameters, such as the height, width and self-weight of the building, the thickness of the liquefiable layers and the magnitude of the peak base acceleration. The results obtained can be used to analyse and design buildings built on foundation ground susceptible to liquefaction.

2. Background of Effective Stress Analysis Program

There is no doubt that a capable numerical effective stress analysis that is well-calibrated and executed provides the most realistic simulation of the liquefaction process. For this purpose, the computer program FLIP (Finite Element Analysis of Liquefaction Process) was used. The FLIP program was originally developed in Japan by Port and Harbour Research Institute, Ministry of Transport (currently Port and Airport Research Institute) [15] and advanced through the cooperative efforts with Kyoto University and Coastal Development Institute of Technology. The program, especially formulated for dynamic effective stress analysis of soil-structure systems during earthquakes, including soil liquefaction, has been well-validated using Japanese earthquake case histories and has been applied to design many waterfront structures in Japan [16].

The advanced version of FLIP program has a two-dimensional effective stress analytical scheme that allows redistribution and dissipation of excess pore water pressures based on the constitutive model called *cocktail glass model*. The model assumes that a granular material consists of an assemblage of particles with contacts either newly forming or disappearing, changing the micromechanical structures during macroscopic deformation. These structures are idealized through a strain space multiple mechanism model as a two-fold structure consisting of a multitude of virtual two-dimensional mechanisms, each of which consists of a multitude of virtual simple shear mechanisms of one-dimensional nature. In particular, a second-order fabric tensor describes direct macroscopic stress–strain relationship, and a fourth-order fabric tensor describes incremental relationship.

In this framework of modeling, the mechanism of interlocking defined as the energy-less component of macroscopic strain provides an appropriate bridge between micromechanical and macroscopic dilative component of dilatancy. Another bridge for contractive component of dilatancy is provided through an obvious hypothesis on micromechanical counterparts being associated with virtual simple shear strain. It is also postulated that the dilatancy along the stress path beyond a line slightly above the phase transformation line is only due to the mechanism of interlocking and increment in dilatancy due to this interlocking eventually vanishing for a large shear strain. These classic postulates form the basis for formulating the dilatancy in the strain space multiple mechanism model. Further details of this model are presented by Iai et al. [17].

3. Model verification of centrifuge tests

3.1 Determination of Soil Parameters

Before proceeding with the investigation of the parameters affecting liquefaction-induced settlements, the scheme adopted was first validated through the results of centrifuge tests available in the literature. For this purpose, the centrifuge tests carried out by Dashti et al. [4] was numerically simulated using the program FLIP. Among the centrifuge tests reported, the 1-D test on T3-50-SILT was selected, where the soil profile consists of the following (from the top to bottom): Monterey Sand (relative density, D_r = 85%, 1.2 m thick), Silica flour (0.8 m thick), Nevada Sand (D_r = 50%, 3 m thick) and Nevada Sand (D_r = 90%, 21 m thick); among these layers, Nevada Sand with D_r = 50% was the liquefiable material.

The static properties of the soils, such as density, porosity, shear modulus and bulk modulus, were all determined as reported by Dashti and Bray [11]. On the other hand, the cyclic/dynamic properties are controlled by parameters that are related to the soil behaviour during the liquefaction. To obtain the dynamic parameters for input in FLIP, the results of undrained cyclic triaxial tests on the soils need to be numerically simulated. However, cyclic triaxial results for Nevada Sand (D_r = 50%) are not available in the literature; as substitute, Christchurch Sand, which has been extensively investigated at the University of Auckland, was used instead. For comparison purposes, the index properties of both Nevada sand and Christchurch sand are summarised in Table 1, while the grain size distribution curves are shown in Figure 1. These properties of Christchurch sand were determined based on methods specified in NZ Standard [18]. Based on these properties, it can be observed that Christchurch sand is a reasonable substitute to Nevada sand.

Some related experimental tests for the geotechnical properties of Christchurch sand such as particle size distribution (PSD) (Fig. 1), specific gravity (G_S), maximum and minimum void ratios (e_{max} and e_{min}) (Table 1) and soil compaction properties were conducted also in accordance with NZS4402 [18].

Table 1 – Index properties of Nevada sand and Christchurch sand.

	Christchurch sand	Nevada sand
Specific gravity, G_s	2.65	2.65 –2.67
Max. void ratio, e_{max}	1.08	~ 0.75 – 0.89
Min. void ratio, e_{min}	0.67	~ 0.49 –0.56

Aside from using Christchurch sand to calibrate the D_r = 50% Nevada sand, this paper used the same parameter values as reported by Dashti and Bray [11] in the numerical simulation using FLIP; the parameters used are summarised in Table 2. In addition to numerically simulating the cyclic resistance curves, other undrained response, such as axial strain development, effective stress path, etc., were matched with the actual experimental results. Fig. 2 provides a representative comparison of the simulated and measured soil response during an undrained cyclic triaxial test on Christchurch sand (cyclic shear stress ratio, *CSR*=0.18).

3.2 Model Description

The configuration of the centrifuge test T3-50-SILT as reported by Dashti et al. [4] is shown in Fig. 3. The thin layer of non- plastic silt (silica flour) was placed on top of the looser layer of Nevada Sand to restrict rapid pore pressure dissipation vertically. In the model, the middle structure represented a 2-story building (height above

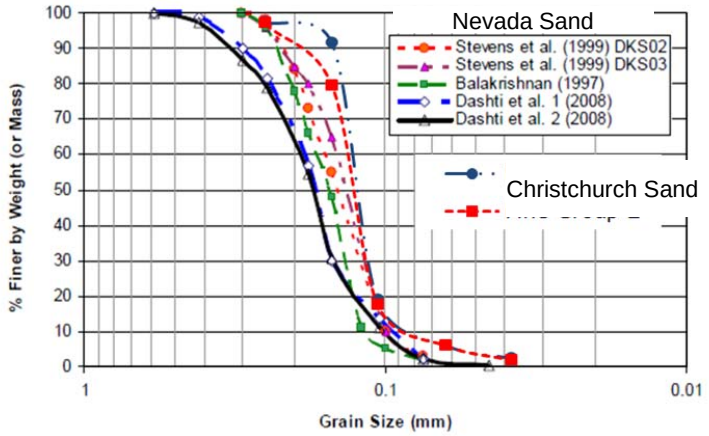

Fig. 1 – Particle size distribution curves of Nevada sand Christchurch sand [4].

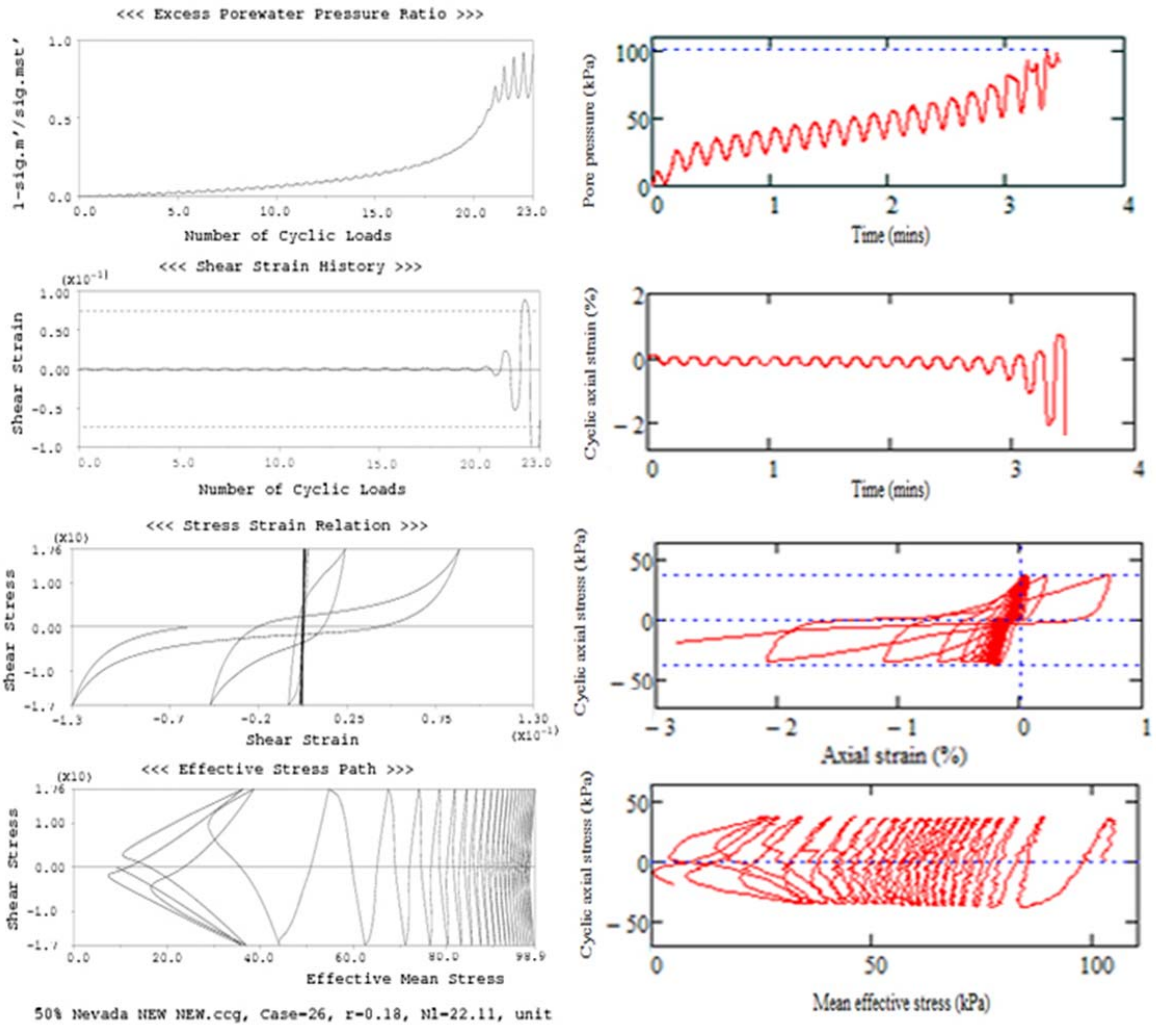

(a) (b)

Fig. 2 – Comparison between (a) simulation; and (b) laboratory cyclic triaxial test results for Christchurch sand (D_r = 50%) at *CSR*=0.18.

Table 2 – Parameters of the four types of soil layers used in the FLIP verification

Parameters		Nevada sand (D_r = 50%)	Nevada sand (D_r = 90%)	Monterey sand (D_r = 85%)	Silica silt
Density ρ (tonne/m^3)		1.63	1.72	1.66	1.67
Porosity n		0.38	0.35	0.36	0.48
Mean eff. conf. pressure (kPa)		100	100	100	100
Initial shear modulus (kPa)		52768	112457	145011	89860
Initial bulk modulus (kPa)		137612	293269	378167	234341
Hydraulic conductivity (m/s)		6×10^{-5}	2.25×10^{-5}	5.29×10^{-4}	3×10^{-8}
Internal friction angle (degree)		34	38	40	33
Phase transformation angle (^{o})		28	29	29	28
Liquefaction parameters for FLIP cocktail glass model*	ε_{dcm}	0.2	0.2	0.08	0.2
	$r_{\varepsilon dc}$	3.6	0.32	0.32	3.6
	$r_{\varepsilon d}$	0.25	0.25	0.25	0.25
	r_k	0.73	0.5	0.11	0.5
	q_1	1	1	1	1
	q_2	0.75	1	1	0.75
	q_4	1	1	1	1

*For details of these parameters used in FLIP, refer to Iai at al. [15]

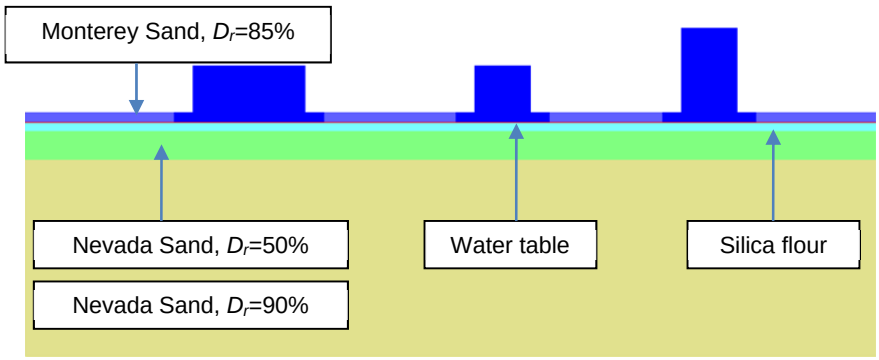

Fig. 3 – Schematic diagram of the centrifuge model test (modified from Dashti et al. [4]).

ground, H=5m) with width B=6m; the left structure had an increased width (B=12m) while the right structure represented a taller 4-story building (B=6m, H=9m). All structural models were single-degree-of-freedom structures with a lumped mass supported by two side columns made of steel, which were placed on a 1m-thick rigid mat foundation made of aluminum. The finite element mesh used in FLIP is illustrated in Fig. 4.

3.3 Verification Results

The results of the centrifuge test using the ground motion recorded at a depth of 83m in the Port Island downhole array during the 1995 Kobe earthquake (with peak base acceleration scaled to 0.55g) as input motion are compared to the FLIP simulation results in terms of the development of excess pore water pressure ratio and vertical displacements. These are discussed below.

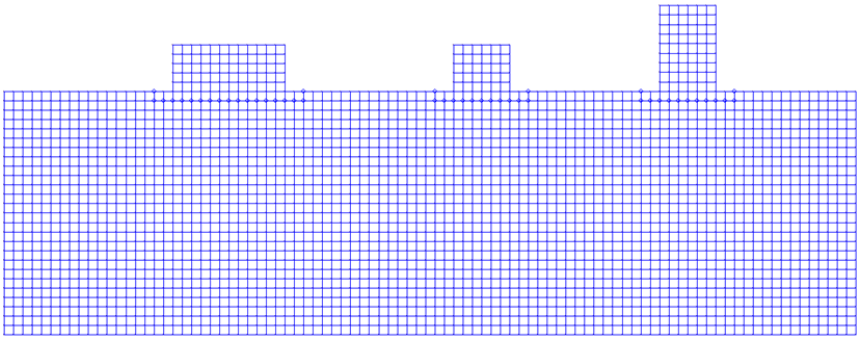

Fig. 4 – Finite element mesh for the centrifuge test simulation.

3.3.1 *Excess Pore Water Pressure (EPWP) Ratio*

The excess pore pressure time histories under each structure obtained by FLIP simulation are compared with the results of the T3-50-SILT centrifuge test results in Fig. 5. When considering the centrifuge results, refer to those for T3-50-SILT test. It is obvious that the excess pore water pressure generated in the numerical simulation was much higher than in the centrifuge test. The hydraulic conductivity, k, for the silt layer (about 3×10^{-8} m/s, as indicated in Table 2), appears to be too low to allow water to be drained out of the ground over in such short period; therefore, high excess pore water pressure is to be expected in the simulation. Note that in the centrifuge test, the 0.8m thickness of silica silt layer may have cracked due to large ground deformation, and allowed the dissipation of excess pore water pressure; such phenomenon is difficult to model numrically.

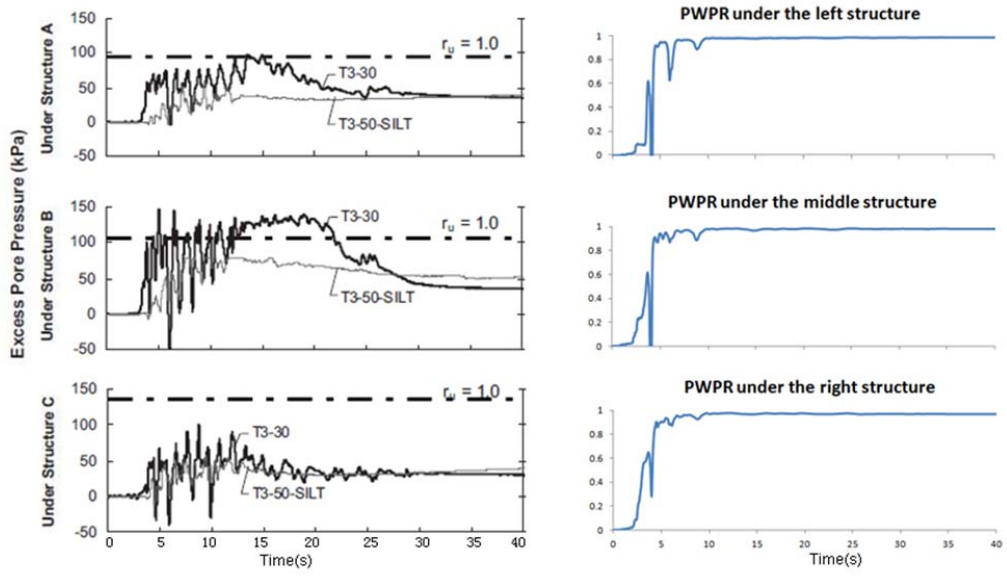

(a) (b)

Fig. 5 – (a) Centrifuge test results; and (b) simulation results showing the development of excess pore water pressure ratio under each structure (Note: centrifuge test results are from Dashti et al. [4]).

3.3.2 *Vertical Displacement*

Next, the vertical displacements under each structure computed using FLIP were compared with the centrifuge test results, and this is shown in Fig. 6. As in the previous sub-section, please refer to the results for T3-50-SILT for the centrifuge test result. From the figure, it can be surmised that the residual vertical displacements of the three structures computed from numerical simulation are roughly the same as those from the centrifuge tests. Moreover, the trends of the vertical displacements of the three structures are also very similar to each other.

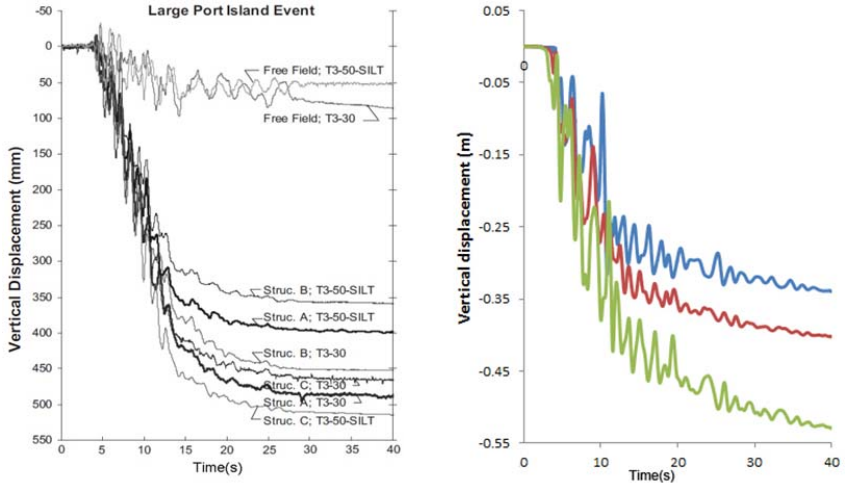

(a) (b)

Fig. 6 – (a) Centrifuge test results; and (b) simulation results showing the development of vertical displacement of each structure (Note: centrifuge test results are from Dashti et al. [4]).

From the observed data, a couple of observations can be highlighted: (1) when two buildings have the same width, the taller building tends to settle more than the shorter one; and (2) when two buildings have the same height, the narrower building will settle more than the wider one. Another observation is that in the relatively "quiet period" after the major shaking (i.e. 15s to 40s), the settlements of the three buildings in the centrifuge test became more or less constant, while the numerical simulation showed continuous increase; in other words, the slopes of the vertical displacement curves in the simulation are a bit higher than the ones in the centrifuge test. A possible reason for this is the quick dissipation of EPWP in the centrifuge test (refer to Fig. 5); after t=15s, the EPWP ratios are almost less than 0.5, indicating that at least half of the effective stress has been restored and, as result, the deformations in the "quiet period" contributed little to the total settlement.

3.3.3 *Summary of Verification Exercise*

The numerical simulation of the centrifuge experiment conducted by Dashti et al. [4] showed satisfactory match, demonstrating that the FLIP effective stress computer program can reasonably mimic the liquefied soil-structure interaction during large earthquakes. The simulation model will then be used to investigate the effects of various parameters on the overall response of buildings constructed on liquefiable ground.

4. Parametric Studies

In this section, the effects of various geometric/earthquake properties on the seismic performance of buildings on liquefiable soil are investigated. Here, only the effects of the following parameters are presented: (1) height of building; (2) width of footing; (3) peak base acceleration; and (4) thickness of liquefiable layer. Note that the peak acceleration at the ground surface is difficult to control as it is affected by the soil properties; thus, peak base acceleration (maximum amplitude of input motion at the bedrock) was selected as an alternative instead. Due to space limitation, only the results of the parametric studies using a specified time history of motion is presented; more simulations are planned to assess the response of the model ground to other motions.

4.1 Input Motion

The input base motion selected is a stochastically generated ground motion; this was adopted so that the characteristics of the motion can be easily controlled in the analysis [19]. In FLIP, the horizontal acceleration is applied at the base of the soil profile, which is assumed to be the top of the bedrock. Therefore, the motion selected was generated to fit the shape of spectra for soil site Class A and B (strong rock and rock) as specified in the New Zealand Design Standard [20]. The input acceleration and its response spectrum are plotted in Fig. 7.

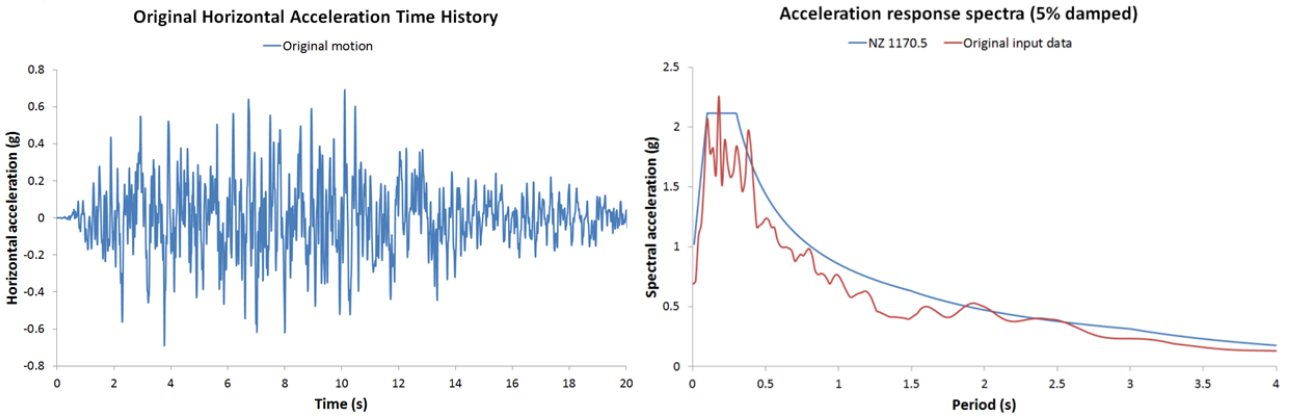

(a) (b)

Fig. 7 – Characteristics of the input acceleration used: (a) time history; and (b) response spectrum at 5% damping and the NZS design spectrum for Class A and B sites.

4.2 Soil Profile

The soil profile used in the parameteric study is shown in Fig. 8. The model consists of three layers: 2m thick dense crust; 3m thick liquefiable layer; and 21m thick dense base layer. The dense materials used in the crust and base layer are the same, i.e. Nevada sand with D_r = 90%. Similarly, the liquefiable layer is Nevada sand (with liquefaction properties of Christchurch sand) with D_r = 50%. These have been discussed in the previous section.

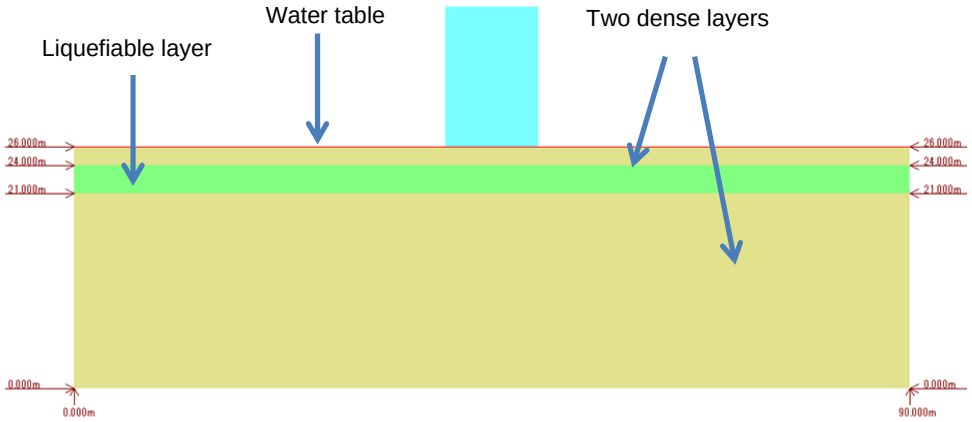

Fig. 8 – Cross-section of the model ground used in parametric study.

Note that in dynamic problems, the boundary conditions are quite important because they may not allow the necessary energy dissipation and can result in the reflection of outward propagating waves back into the model. In this study, a wide model is used to minimize the problem, since material damping will absorb most of the energy in the waves reflected from distant boundaries. Also, roller boundaries are assigned along the sides of the model, and a fixed boundary along the base.

4.3 Results of Parametric Studies

4.3.1 *Effect of Structure Height/Width Ratio*

The effect of the aspect ratio (i.e., ratio of structure height to width) has been investigated and the results are shown in Fig. 9. In Fig. 9(a), it is clear that the normalised settlement (S/H_L), that is, the vertical settlement, S, normalised by the thickness of liquefiable layer, H_L, increases with the aspect ratio, H/B. The results are consistent with what is expected, i.e. the settlement of the building will increase with an increase in height or decrease in width of the building.

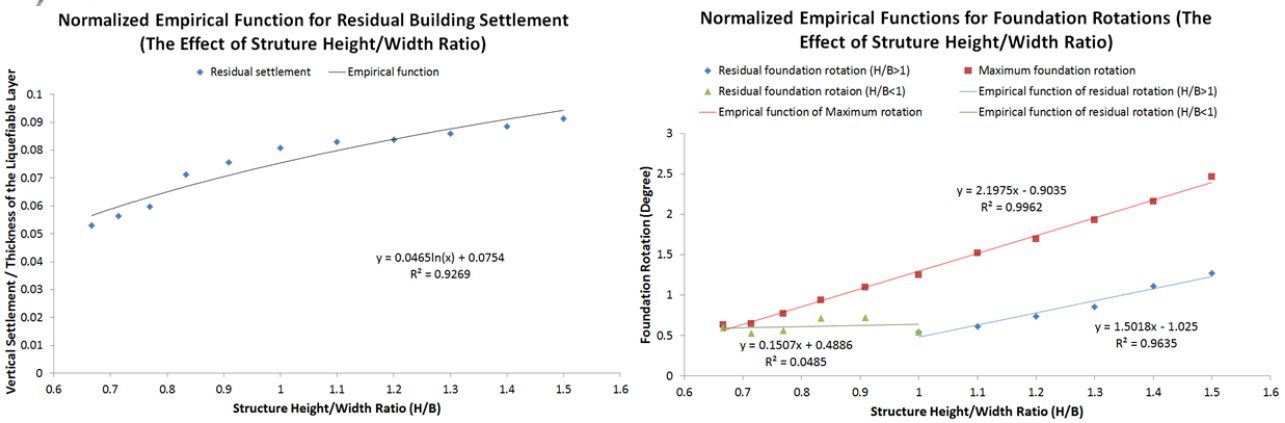

(a) (b)

Fig. 9 – Relation between the structure aspect ratio and (a) normalised settlement; and (b) foundation rotation.

In addition to building settlement, foundation rotation (or tilt of the building) is another problem associated with earthquake-induced building movements. Fig. 9(b) summarises the relations between the *H*/*B* ratio and maximum or residual foundation rotation. These tilts are induced by the directionality of earthquake motion; irregular building geometry can induce further tilt (but this is out of scope in this study). The maximum foundation rotation, θ_{max}, increases linearly with the increase in the aspect ratio (*H*/*B*). However, the relation between *H*/*B* and residual foundation rotation, θ_{res} appears to be bilinear, i.e., when the $H/B < 1$, θ_{res} is almost constant with value close to 0.5°; on the other hand, when the $H/B > 1$, θ_{res} increases linearly with *H*/*B*. As *H*/*B* approaches 0.7 or less, θ_{res} becomes similar to θ_{max}. This may be an artefact of the thickness of the liquefiable layer used; more simulations are needed to confirm this trend.

It is clear that with the increase in building height (assuming the building width remains constant), the liquefaction-induced building settlement and foundation rotation increased. As explained by Dashti et al. [4], increasing either the structure height/width ratio (*H*/*B*) or the building weight would result in a huge increase in the soil-structure interaction(SSI)-induced building ratcheting due to the cyclic loading of foundation (ε_q-SSI). The SSI-induced cyclic loading of the foundation can result in shear-induced structural settlements, i.e. the appropriate mechanism is as follows: the uplift of foundation edge disturbs the soil underneath it, and then in the next cycle, the downward loading at this location induces more settlement. In addition, the three other strain sources mentioned by Dashti et al. [4], namely, ε_p-DR (localized volumetric strains due to partial drainage), ε_p-CON (consolidation due to excess pore pressure dissipation) and ε_q-BC (partial bearing failure due to the strength loss in the foundation soil) will also increase and contribute to the building movement.

With the increase in building width, both vertical settlement and foundation rotation decreased. In this case, a huge decline in ε_q-SSI would occur, while the ε_p-DR would likely follow a downward trend. Even if the increase in ε_p-CON and ε_q-BC is considered with the change, the total settlement would be affected more by the decrease in ε_q-SSI and ε_p-DR. Furthermore, by decreasing the structure height/width ratio (*H*/*B*), the contribution of ε_q-SSI would drop significantly. The decrease in vertical displacement and foundation rotation angle in Fig. 9 confirmed this observation. However, the building weight is increased with the increase in both building height and width; the increase in building weight in both situations would lead to opposite response in building movements. This indicates clearly that the building weight cannot be seen as a factor separately but should be considered with other factors, such as the height/width ratio (*H*/*B*) and the density of the building.

4.3.2 *Effect of Peak Base Acceleration*

Fig. 10(a) shows the relation between the normalised settlement and the amplitude of the peak base acceleration. It is noted that the trend is linear; with increasing intensity of shaking, the settlement of the building increases. On the other hand, as shown in Fig. 10(b), the maximum and residual foundation rotation appears to be a power function of the peak base acceleration, with a higher rate of change as the acceleration value increases.

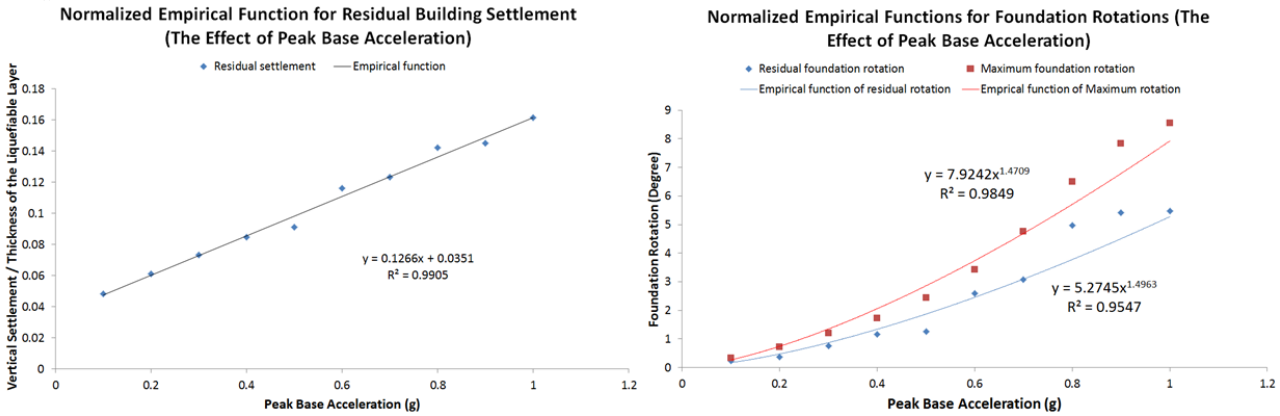

(a) (b)

Fig. 10 – Relation between the peak base acceleration and: (a) normalised settlement; and (b) foundation rotation.

The major reason for this phenomenon is the SSI effect. Dashti et al. [4] suggested that with the increase in the amplitude of the peak base acceleration, all four types of strains (ε_p-DR, ε_p-CON, ε_q-BC and ε_q-SSI) would increase significantly. In the simulation presented herein, there is no "quiet period" in the input motion and consequently, the effects of ε_p-CON could not be quantified. Therefore, the increase in building settlement and foundation rotation can be considered to be the mutual action of ε_p-DR, ε_q-BC and ε_q-SSI generation.

4.3.2 *Effect of Thickness of Liquefiable Layer*

Finally, the effect of the thickness of liquefible layer is investigated. Liu & Dobry [10] have developed a chart showing the relationship between building settlement and building width, both normalised by the thickness of liquefiable layer. However, Dashti et al. [4] have indicated that the chart is misleading in terms of understanding the structural response when the liquefiable layer is thin. In the present numerical simulations, the 2m thick dense crust and the total depth of the profile (26m) were maintained constant. The liquefiable layer thickness was increase from 3m to 10m; consequently, the depth of the dense base layer was decreased from 21m to 14m.

The results of all the numerical simulations conducted in Sections 4.3.1 and 4.3.3 are incorporated in the chart revised by Dashti et al. [4] and reproduced in Fig. 11. A new upper bound needs to be re-defined to account for the data obtained when the building width is greater than three times the liquefiable depth.

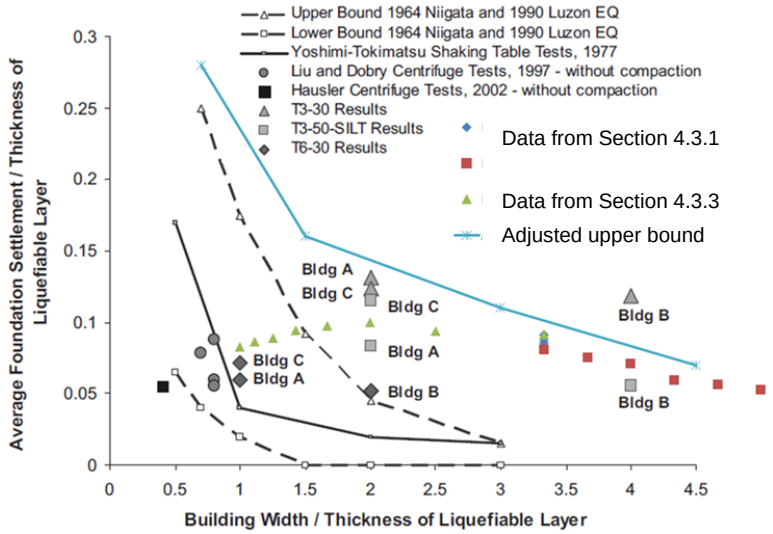

Fig. 11 – Updated normalised foundation settlement chart (revised from [4]).

5. Concluding Remarks

Understanding the mechanisms of liquefaction-induced building movements is of great significance to geotechnical engineers in order to mitigate the hazards to buildings caused by large earthquakes. However, there is insufficient research on this subject, especially concerning the fundamental mechanisms of building movements during liquefaction. In addition, currently available empirical formulas developed for free field conditions would not be suitable to estimate liquefaction-induced building movements. Based on the previous researches and case studies, the observations that have been presented in this paper provided insightful explorations of the above issues.

In the verification stage, through a series of laboratory experiments and literature review, the static and dynamic parameters of various materials adopted in the FLIP program were determined. The use of the finite element analysis tool, FLIP, to solve liquefaction-related issues has been validated by simulating centrifuge experiment and comparing the results with the numerically-derived measurements. Next, the effects of various parameters, in terms of building aspect ratio, peak base acceleration and liquefiable layer thickness, on building settlements were examined. Clear trends of building settlements and foundation rotation were observed.

The results of the parametric study illustrated that taller buildings experience stronger rocking and generate larger vertical stress than shorter buildings and, with the increase in building height, liquefaction-induced building settlement and foundation rotation worsened. Moreover, it was found that both vertical settlement and foundation rotation decrease with the increase in building width. In addition, while the normalised settlement increased linearly with the peak base acceleration, both the maximum and residual foundation rotation appear to increase dramatically with the peak base acceleration.

Note that in the results presented herein, only one time history of motion was used in the analyses (even when investigating the effect of peak base acceleration analysis, the motions used were developed by scaling the motion); therefore, trends discussed here can be said to be valid only for this motion. In the future, the results of the analyses using other input motions will be reported to elucidate the more general response of the building in a liquefiable ground.

6. Acknowledgment

The authors would like to thank Prof S. Iai of Kyoto University and the FLIP Consortium for the use of the computer program employed in this research.

7. References

[1] Day RW (2002): Geotechnical Earthquake Engineering Handbook. McGraw-Hill, New York, NY.

[2] Towhata I (2010): *Geotechnical Earthquake Engineering*. Springer Science & Business Media.

[3] Kramer SL (1996): *Geotechnical Earthquake Engineering*. Prentice Hall, Upper Saddle River, NJ.

[4] Dashti S, Bray J, Pestana J, Riemer M, Wilson D (2010): Mechanisms of seismically induced settlement of buildings with shallow foundations on liquefiable soil. *Journal of Geotechnical and Geoenvironmental Engineering*, 136(1), 151–164.

[5] Seed RB, Cetin KO, Moss RE, Kammerer AM, Wu J, Pestana JM, Riemer MF, Sancio RB, Bray JD, Kayen RE (2003): Recent advances in soil liquefaction engineering: a unified and consistent framework. *Proceedings of the 26th Annual ASCE Los Angeles Geotechnical Spring Seminar*: Long Beach, CA.

[6] Youd T, Idriss I, Andrus R, Arango I, Castro G, Christian J, Dobry R, Finn W, Harder L Jr, Hynes M, Ishihara K, Koester J, Liao S, Marcuson W III, Martin G, Mitchell J, Moriwaki Y, Power M, Robertson P, Seed R, Stokoe K II (2001): Liquefaction resistance of soils: summary report from the 1996 NCEER and 1998 NCEER/NSF Workshops on evaluation of liquefaction resistance of soils. *Journal of Geotechnical and Geoenvironmental Engineering*, 127(10), 817–833.

[7] Byrne PM, Park SS, Beaty M, Sharp M, Gonzalez L, Abdoun T (2004): Numerical modeling of liquefaction and comparison with centrifuge tests. *Canadian Geotechnical Journal*, 41(2), 193-211.

[8] Lopez-Caballero F, Farahmand-Razavi AM (2008): Numerical simulation of liquefaction effects on seismic SSI. *Soil Dynamics and Earthquake Engineering*, 28(2), 85-98.

[9] Hausler EA (2002): Influence of ground improvement on settlement and liquefaction: A study based on field case history evidence and dynamic geotechnical centrifuge tests. *PhD Thesis*, University of California, Berkeley.

[10] Liu L, Dobry R (1997): Seismic response of shallow foundation on liquefiable sand. *Journal of Geotechnical and Geoenvironmental Engineering*, 123(6), 557–567.

[11] Dashti S, Bray JD (2013): Numerical simulation of building response on liquefiable sand. *Journal of Geotechnical and Geoenvironmental Engineering*, 139(8), 1235-1249.

[12] Elgamal A, Lu J, Yang Z (2005): Liquefaction-induced settlement of shallow foundations and remediation: 3D numerical simulation. *Journal of Earthquake Engineering*, 9(spec01), 17-45.

[13] Popescu R, Prevost JH (1993): Centrifuge validation of a numerical model for dynamic soil liquefaction. *Soil Dynamics and Earthquake Engineering*, 12(2), 73-90.

[14] Shahir H, Pak A (2010): Estimating liquefaction-induced settlement of shallow foundations by numerical approach. *Computers and Geotechnics*, 37(3), 267-279.

[15] Iai S, Matsunaga Y, Kameoka K. (1992): Strain space plasticity model for cyclic mobility. *Soils and Foundations*, 32(2), 1-15.

[16] FLIP Consortium (2011): FLIP: Examples of applications, http://flip.or.jp/e_examples.html

[17] Iai S, Tobita T, Ozutsumi O, Ueda K (2011): Dilatancy of granular materials in a strain space multiple mechanism model. *International Journal for Numerical and Analytical Methods in Geomechanics*, 35(3), 360-392.

[18] Standards New Zealand (1986): Methods of testing soils for civil engineering purposes. *NZS 4402:1986*, Standards New Zealand.

[19] Bi K, Hao H (2012): Modelling and simulation of spatially varying earthquake ground motions at sites with varying conditions. *Probabilistic Engineering Mechanics*, 29, 92-104.

[20] Standards New Zealand (2004). Structural design actions - Part 5: Earthquake actions - New Zealand Commentary. *NZS 1170-5* (S1), Standards New Zealand.